

Atomic silicon towards the Orion-KL nebula^{*}

C. Gry¹, G. Pineau des Forêts², and C.M. Walmsley³

¹ ISO Data Centre, ESA Astrophysics Division, Villafranca del Castillo, P.O.Box 50727, E-28080 Madrid, Spain

² Observatoire de Paris, F-92195 Meudon Principal Cedex, France

³ Osservatorio Astrofisico di Arcetri, Largo E. Fermi 5, I-50125 Firenze, Italy

Received 8 April 1999 / Accepted 7 June 1999

Abstract. We have used the Long Wavelength Spectrometer (LWS) on board ISO to observe the fine structure lines of atomic silicon at 68.5 and 129.7 microns towards the Orion Kleinmann-Low nebula. Our data show evidence for the detection of the $J=2-1$ transition at $68.5\mu\text{m}$ with a signal-to-noise ratio of 5. We consider the formation of the observed emission line and conclude that it is likely to form in the C-shock associated with the outflow emanating from the young massive stars in that complex. We give limits on the shock velocity and magnetic field required to explain the observed line in this manner.

Key words: ISM: abundances – ISM: H II regions – ISM: individual objects: Orion-KL nebula – ISM: jets and outflows

1. Introduction

The fine structure lines of neutral atomic silicon at 129.68 ($J=1-0$) and 68.47 microns ($J=2-1$, wavelengths measured by Brown et al., 1994, see Fig. 1) have not to our knowledge been observed in the interstellar medium. They are however analogous to the well known lines of atomic carbon (609 and $370\mu\text{m}$) and atomic oxygen (63 and $145\mu\text{m}$). They also are interesting in that they trace silicon which is thought to be one of the main elements involved in interstellar dust grains. A detection of the [Si I] lines would therefore be of considerable significance as a tracer of conditions in the interstellar medium as well as being a first astronomical detection.

Where does one expect to find the [Si I] lines? The most obvious answer to this question would seem to be in regions where the $35\mu\text{m}$ transition of Si^+ has been detected; that is towards the Orion Bar PDR or towards the shocked gas in Orion-KL (Haas et al. 1991). These authors find an abundance for Si II of roughly ten percent solar corresponding to a column density of order 10^{16} cm^{-2} . It seems reasonable as a first guess to suppose that the atomic Si abundance may be similar. With

Send offprint requests to: M. Walmsley

^{*} Based on observations with ISO, an ESA project with instruments funded by ESA Member States (especially the PI countries: France, Germany, the Netherlands and the United Kingdom) with the participation of ISAS and NASA

Correspondence to: walmsley@arcetri.astro.it

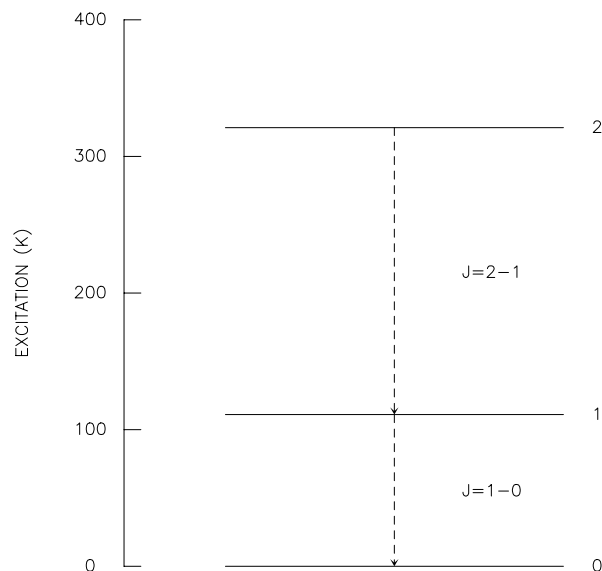


Fig. 1. Energy Level diagram for the ^3P ground state of Si I. The Einstein A-coefficients are $8.3 \cdot 10^{-6}\text{ s}^{-1}$ for the 1-0 transition and $4.2 \cdot 10^{-5}\text{ s}^{-1}$ for the 2-1 transition.

this in mind, we attempted to detect the two [Si I] lines using the ISO Long wavelength spectrometer (LWS).

2. Observations

We performed LWS Fabry-Perot scans around the $68.5\mu\text{m}$ and $129.7\mu\text{m}$ [Si I] lines, with 7 spectral elements on each side of the lines and an oversampling of 4 and 30 sec integration time per point resulting in 60 scans for each line. The spectral resolutions are respectively of order $0.0084\mu\text{m}$ and $0.014\mu\text{m}$ (Trams et al., 1996).

The observations originally processed with version 7.0 of the ISO-LWS Off Line Processing software, have been further processed with the LWS Interactive Analysis software LIA 7.1 (partly to improve the dark current subtraction). Fabry-Perot observations are also contaminated by contribution from neighbouring orders and by straylight (the intensity of which varies with source and wavelength). To correct for this, we normalize the continuum to that derived from an LWS grating observation of the same region obtained in the central

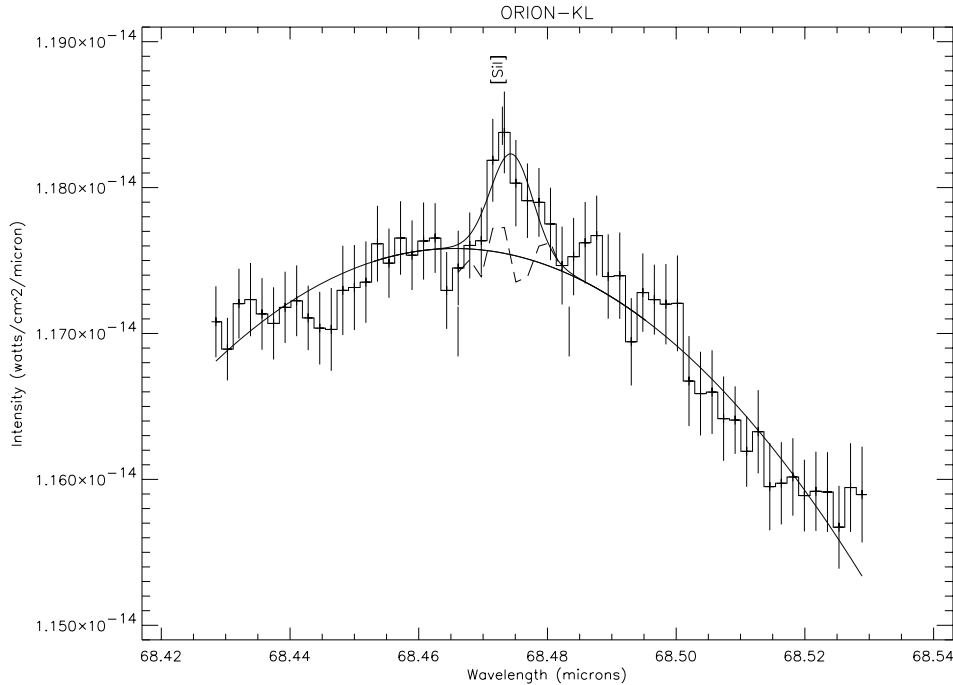


Fig. 2. Spectrum of the Si I $68.5 \mu\text{m}$ line observed with the LWS Fabry-Perot (histogram). The continuum has been scaled to the value measured with the grating in order to correct for straylight and/or contamination by other orders. The solid line superposed represents a fit by a second-order-polynomial baseline and a gaussian which has the width of the instrumental resolution. The dashed line represents the residuals of the gaussian line fit.

program of the LWS Consortium; after applying the strong source correction, the grating observations give intensities respectively of $1.18 \cdot 10^{-14} \text{ W cm}^{-2} \mu\text{m}^{-1}$ at $68 \mu\text{m}$ and $8.8 \cdot 10^{-16} \text{ W cm}^{-2} \mu\text{m}^{-1}$ at $129 \mu\text{m}$. With these corrections, the photometric accuracy is considered to be 30%.

The signal to noise ratio achieved on the continuum at $68.5 \mu\text{m}$ is over 500. At $129 \mu\text{m}$, data are affected by high frequency fringing and this effect essentially determines our current achievable sensitivity at this wavelength.

To convert our observed line fluxes to an intensity scale, we used the beam profile FWHM values listed in Swinyard et al. (1998): $81.5'' \times 84.5''$ at $68 \mu\text{m}$, and $78.1'' \times 74.9''$ at $129 \mu\text{m}$.

3. Results

In Fig. 2, we show our spectrum of the $68.5 \mu\text{m}$ line corrected as explained in Sect. 2. The apparent curvature of the continuum is due to a residual in the correction for the grating resolution element profile.

The most interesting feature of this spectrum is the presence of a narrow feature at the expected frequency with a full width at half maximum compatible with the spectral resolution and an intensity of $6.1 (\pm 2.5) \cdot 10^{-19} \text{ W cm}^{-2}$. The intensity has been measured by integrating the flux above a fitted baseline and the uncertainty includes the range of values obtained using different possible baselines. Although the FP instrumental profile is not gaussian, we get the same result by fitting a gaussian as shown for comparison on Fig. 2. We note also the presence in our spectrum of a “broad” feature with width roughly 200 km s^{-1} centred at the [Si I] line frequency. It is quite possible that this has an instrumental origin but we note here merely that it is consistent with an origin in the Orion outflow (see e.g. Blake et al. 1987) and that the integrated intensity if real might be as

much as a factor 2 larger than the “narrow” feature discussed above.

For a beam of $81.5'' \times 84.5''$, the observed flux in the narrow feature corresponds to a line intensity of $4.8 (\pm 2) \cdot 10^{-5} \text{ erg s}^{-1} \text{ cm}^{-2} \text{ sr}^{-1}$. We have attempted to verify the reality of this feature by dividing our data into two halves and comparing the results. These are reasonably consistent with one another and hence we think that we have detected Si I emission. However, quite clearly, independent verification is needed.

In our spectrum of the $129.7 \mu\text{m}$ feature on the other hand, we observe no feature above a limit of $1.1 \cdot 10^{-5} \text{ erg s}^{-1} \text{ cm}^{-2} \text{ sr}^{-1}$. This corresponds to a limit on the line intensity ratio $I(129)/I(68)$ of 0.23.

4. Physical parameters in the region emitting [Si I]

We have made simple level population estimates for [Si I] in order to translate the observed line intensity into a column density $N(\text{Si I})$. We can also use the limit on $I(129)/I(68)$ to derive a lower limit to the temperature of the region emitting the $68.5 \mu\text{m}$ line. We have used for this purpose CI collisional rates (Schroeder et al. 1991) and the Einstein A-values given by Brown et al. (1994). The “critical” densities computed in this way (for $T=500 \text{ K}$) are 10^5 cm^{-3} and $2 \cdot 10^5 \text{ cm}^{-3}$ for the 129 and $68 \mu\text{m}$ lines respectively. These values are less than current estimates for the density of the gas in Orion-KL and the surroundings (upwards of 10^5 cm^{-3}) and we hence expect the Si I level populations to be close to being thermalised.

In Fig. 3, we show the expected intensity ratio of the 129 and $68 \mu\text{m}$ lines as a function of temperature for three densities which bracket the values expected in Orion-KL. We see that the observed upper limit of 0.23 to $I(129)/I(68)$ implies a lower limit on the temperature of the region emitting the $68 \mu\text{m}$ line of

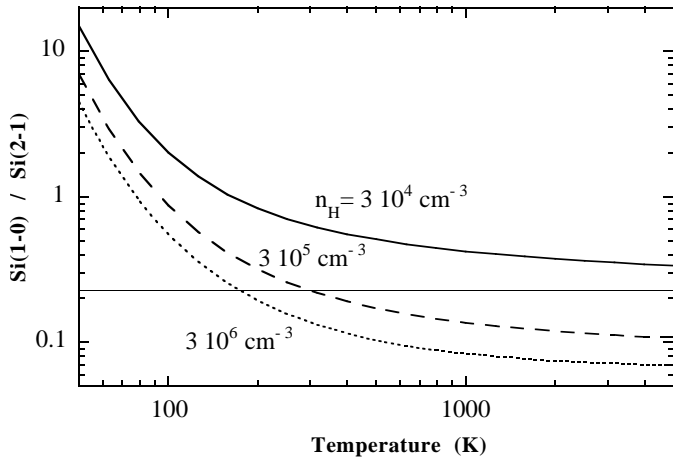


Fig. 3. Intensity ratio of the $129\mu\text{m}$ to $68\mu\text{m}$ Si I lines as function of temperature for densities of $3 \cdot 10^4 \text{ cm}^{-3}$ (full line), $3 \cdot 10^5 \text{ cm}^{-3}$ (dashed), $3 \cdot 10^6 \text{ cm}^{-3}$ (dots). The horizontal thin line shows our observed upper limit to the intensity ratio. We infer from this that the temperature in the region where the $68\mu\text{m}$ line is emitted must exceed 200 K.

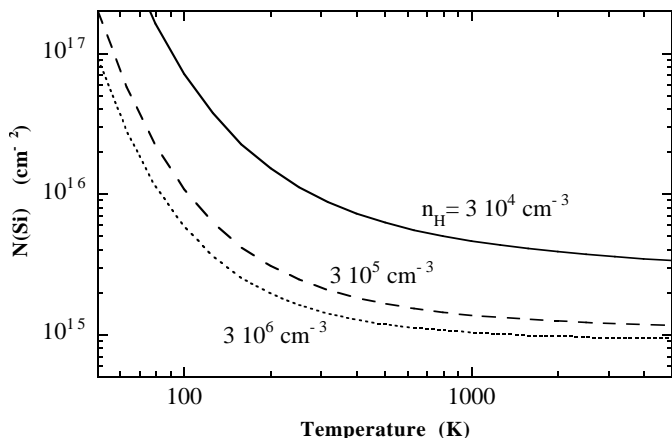


Fig. 4. Inferred column density of Si I towards Orion on the basis of the observed $68\mu\text{m}$ Si I line. Results are given as function of temperature for densities of $3 \cdot 10^4 \text{ cm}^{-3}$ (full line), $3 \cdot 10^5 \text{ cm}^{-3}$ (dashed), $3 \cdot 10^6 \text{ cm}^{-3}$ (dots).

200 K. One sees also that due to the thermalisation of the level populations, the line intensity above densities of $3 \cdot 10^5 \text{ cm}^{-3}$ is only dependent on temperature and column density. Hence, one can use the observed $68.5\mu\text{m}$ line intensity to derive the atomic Si column density as a function of temperature.

The result of this computation is shown in Fig. 4 where one sees that if (as we expect), the density is of order $3 \cdot 10^5 \text{ cm}^{-3}$ or larger, then the atomic silicon column density implied by our observed $68\mu\text{m}$ intensity is in the range $N(\text{Si I}) \sim 1 - 3 \cdot 10^{15} \text{ cm}^{-2}$. This can be compared with the estimate of Haas et al. (1991) of $N(\text{Si II}) = 7 \cdot 10^{15} \text{ cm}^{-2}$ (where we consider the excess emission after a PDR component has been subtracted) and the result of Blake et al. (1987) who find $N(\text{SiO}) = 1.5 \cdot 10^{15} \text{ cm}^{-2}$. Here, one must remember that the ISO aperture (of order $80''$) is roughly a factor two larger than in the measurements of SiO and Si II ($30-40''$). Moreover, high angular resolution SiO maps

(Wright et al. 1996) show that in the J=2-1 transition, there is an extremely bright core (on the arc second scale) surrounded by more extended emission on the scale of 20 arc seconds. Thus, one can guess that the observed [Si I] emission likely comes from a region $20''$ or less in size and that there is an unknown beam dilution which one should take into account when comparing column densities. Nevertheless, one can conclude that within the considerable uncertainties, the column densities of Si I, Si II and SiO towards Orion-KL are comparable with one another.

5. Discussion

5.1. The origin of the Si I emission

The Orion-KL region is extremely complex and it is by no means clear where the observed [Si I] emission is produced. Here, we merely summarize some of the possibilities.

It is known that some of the observed [Si II] emission in this direction forms in the photo-dissociation region (PDR). Haas et al. (1991) have considered this and conclude that roughly 50 percent of the observed [Si II] towards Orion-KL forms in the PDR and the rest is due to shocked gas. We (Walmsley et al. 1999, hereafter WPF) have constructed models of the [Si II] and SiO emission towards the Orion Bar. We conclude that models which explain the observed low level emission of SiO towards the Bar predict also low column densities of [Si I] (typically less than 0.1 percent of [Si II]). We suspect that the PDR towards Orion-KL is similar in many respects to the Orion Bar with the difference that the Bar is observed almost edge on. We therefore conclude that the PDR layer towards KL is probably not the origin of the observed [Si I] emission.

Another possibility might be that the line arises in the “hot core” material which is observed in highly excited molecular emission (see e.g. Kaufman et al. 1998, Wright et al. 1992) and is thought to be heated by young newly formed stars such as Orion-Irc2. The temperature in this region is estimated to be of order 150–200 K and the density above 10^7 cm^{-3} . Thus any atomic silicon emission should be in LTE. Averaged over the ISO beam, we estimate the hot core hydrogen column density to be of order 10^{23} cm^{-2} and the corresponding column density of Si in all forms to be of order $3 \cdot 10^{18} \text{ cm}^{-2}$. This is 3000 times greater than our estimate of the required Si I column density to explain the observed line and hence we cannot exclude the possibility of a hot core contribution. On the other hand, the evidence suggests that refractory elements are almost completely in solid form in the hot core (see e.g. Blake et al. 1987, Turner 1991) and SiO towards Orion-KL does not seem to come from the hot core (Wright et al. 1996). Hence, we consider the “hot core hypothesis” to be unlikely.

This leaves the possibility that the observed $68\mu\text{m}$ feature forms in shocked gas. Neufeld & Dalgarno (1989a,b; see also the discussion of Hollenbach & McKee 1989) have constructed a model which accounts for much of the observed characteristics of the line spectrum observed towards Orion-KL. Among other things, they account for the fifty percent of the [Si II] emission which does not originate in the PDR. They find (based

on earlier work by Draine et al. (1982) and by Chernoff et al. (1982)) that explaining the observations requires both a J-shock (at velocities of order 80 km s^{-1} propagating into the wind) and a C-shock propagating at around 35 km s^{-1} into the ambient gas. The Neufeld-Dalgarno model explains the “excess [Si II] emission” (ie that not produced in the PDR) as forming in the 80 km s^{-1} J-shock where silicon is required to have an abundance of 40 percent of solar. In this model, atomic silicon is rapidly photoionized by the UV photons produced in the shock and the Si I abundance (see Fig. 6 of Neufeld & Dalgarno 1989a) is expected to be roughly 10^{-3} of the total Si abundance. This would cause the fine structure line emission of Si I to be inobservable.

Another possibility for [Si I] is that the observed emission is produced in the C-shock expected to propagate with velocities of around 35 km s^{-1} . Schilke et al. (1997) have shown that sputtering in C-shocks is capable of producing substantial erosion of Si-containing grains. The silicon thus produced gets rapidly transformed by reactions with O_2 and OH into SiO. However, it seems not unlikely that a substantial fraction of silicon remains in atomic form. In the next section, we discuss some C-shock models which are consistent with those considered by Neufeld and Dalgarno and which appear capable of explaining the observed [Si I] emission.

5.2. C-shock models

We have carried out calculations of the silicon chemistry in a C-shock using the prescription discussed by Schilke et al. (1997). Slight updates to the reaction rates have been introduced (see WPF) and we have used the recently calculated sputtering yields of Field et al. (1997), who compute yields for collisions of heavy ions incident upon quartz (SiO_2). We use a preshock gas composition computed at steady-state for the fractional elemental abundances given by Schilke et al. (1997). The ionization degree, which is a critical parameter in this type of model, is determined by cosmic ray ionization. We have assumed a cosmic ray ionization rate ζ of $5 \cdot 10^{-17} \text{ s}^{-1}$ which corresponds to an ionization degree $n_e/n_H = 10^{-8}$ for $n_H = 5 \cdot 10^5 \text{ cm}^{-3}$.

We have in general carried out calculations for a “standard” model with shock velocity 35 km s^{-1} , pre-shock density $5 \cdot 10^5 \text{ cm}^{-3}$, and magnetic field 707 microgauss. The pre-shock density used here is slightly lower than that found by Draine & Roberge (1982, $7 \cdot 10^5 \text{ cm}^{-3}$). Chernoff et al. (1982) found a better fit for lower densities ($n_H = 2 \cdot 10^5 \text{ cm}^{-3}$) and so we show also results for a model with $n_H = 10^5 \text{ cm}^{-3}$. One should note also that when considering pre-shock densities different from the standard case, we have taken $B(\text{microgauss}) = n_H(\text{cm}^{-3})^{0.5}$.

The results of a calculation for the standard case are shown in Fig. 5 where we show the abundances of several species relevant for the silicon chemistry. One sees here the rapid increase of the abundances of Si and SiO in the shock (i.e. coincident with the temperature rise) as well as in the immediate post-shock region due to sputtering of dust grains. This is a consequence of the high relative velocity of neutral species relative to charged grains. One also notes in Fig. 5a however that the [Si I] fine structure

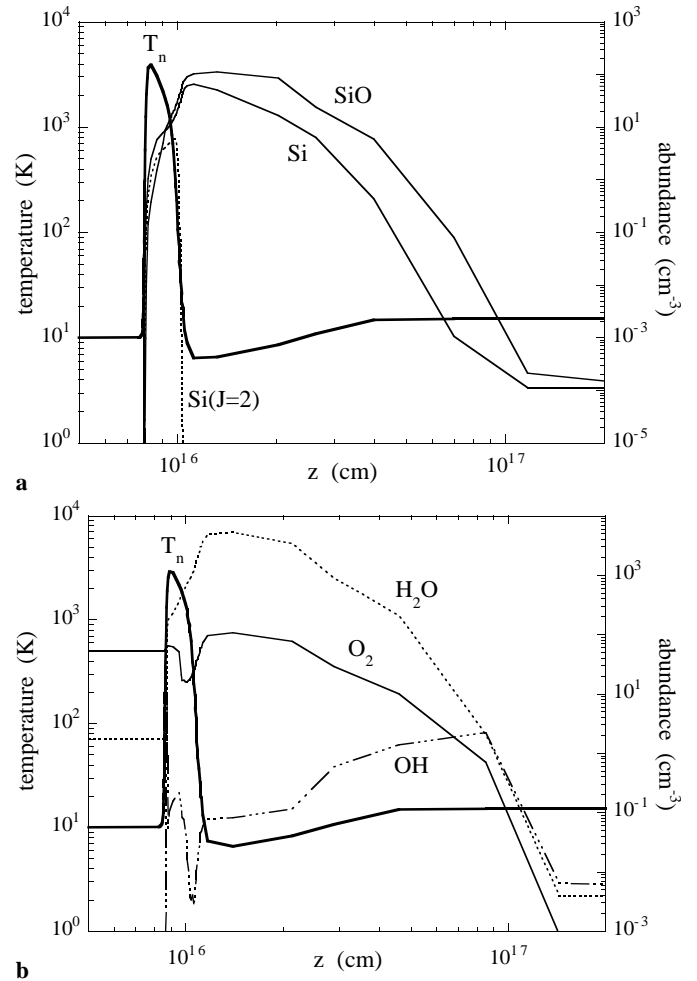


Fig. 5a and b. The upper panel **a** shows the abundances of Si I, Si I(J=2) (dotted line), and SiO computed in our C-shock model plotted as a function of distance along the direction of shock propagation. The temperature of neutral species (bold line) is shown for comparison (left-hand axis). The pre-shock gas is to the left. Calculations are for our standard model with pre-shock density $5 \cdot 10^5 \text{ cm}^{-3}$, shock velocity 30 km s^{-1} , and pre-shock magnetic field $707 \mu\text{G}$. The lower panel **b** shows abundances for O_2 , OH, and H_2O as well as the neutral temperature.

lines will only form in the shock itself where the temperature is above 100 K . Thus while SiO (as well as much of its line emission) may be important in the post-shock gas, the [Si I] lines which are the focus of this paper are specific to the shock itself. Fig. 5b shows the behavior of the abundances of some other species in the shock. Since we assume that the sputtering process produces silicon in atomic form, SiO will be formed by reactions of atomic silicon with OH and O_2 (see e.g. WPF) in the shock and our results suggest that reactions with O_2 will dominate as a rule (though in model 2 discussed below, OH is more important).

In Table 1, we give column densities for several species parallel to the direction of shock propagation as well as the predicted intensity of the J=2-1 [Si I] line.. We have cut off the

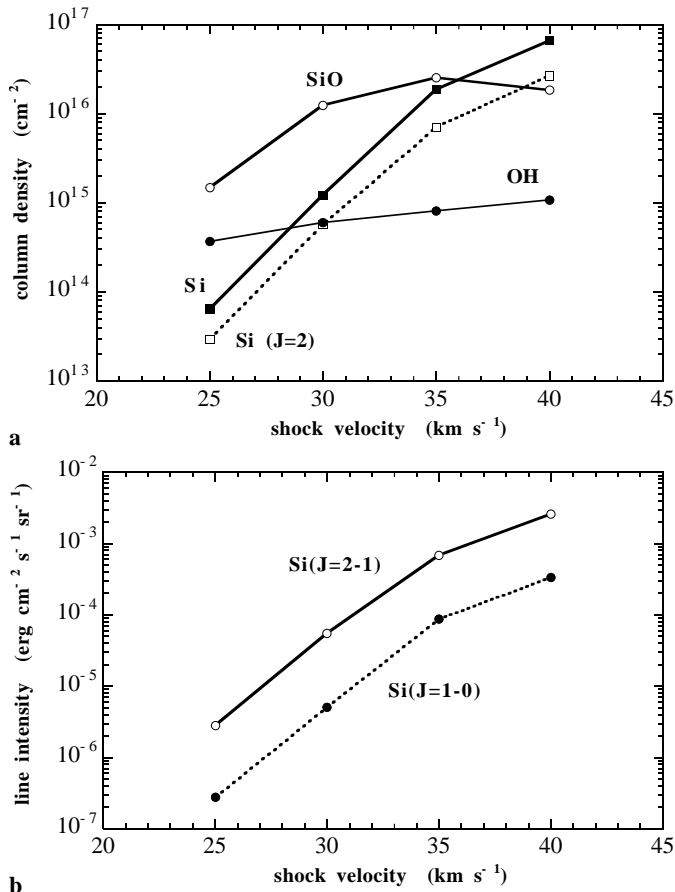


Fig. 6a and b. The upper panel shows the column densities of atomic silicon (Si), SiO, and OH computed by our C-shock models as a function of shock velocity. We have used “standard” parameters of hydrogen nucleon pre-shock density $5 \times 10^5 \text{ cm}^{-3}$ and magnetic field $707 \mu\text{G}$. The lower panel shows predicted line intensities for the same models in the $68 \mu\text{m}$ ($J=2-1$) and $129 \mu\text{m}$ lines.

integration at a temperature of 100 K on the down-stream side of the shock and thus the column densities given in Table 1 refer solely to the hot shocked layer. We note in particular in Table 1 that we have as a rule neglected the possible dissociation of molecules subsequent to collision with grains but in model 2 we have considered this process using the prescription given by Schilke et al. (1997). It is interesting that all of the models in Table 1 explain the observed $J=2-1$ [Si I] line intensity. This comparison is a rough one since we take no account of beam-dilution or inclination effects. Nevertheless, the results suggest that C-shock models of this type are capable of explaining both the atomic silicon and SiO column densities towards Orion-KL. Moreover, the $J=2-1/1-0$ [Si I] intensity ratio predicted by the models is in the range 9–11 for models 1–5 and is 5.6 for model 6. This again is consistent with our limit.

There are still however considerable uncertainties in our C-shock models. As the comparison of models 1 and 2 makes clear, molecular dissociation subsequent to collision with grains may be very important. SiO and H₂O are destroyed in the shock quite

effectively in model 2 leading to a large increase in [Si I]/[SiO]. This is much more apparent in fact than the effect on the H₂O and CO column densities themselves. Thus a more detailed understanding of silicon chemistry in shocks requires reliable estimates of the probability of dissociation due to collision with grains. We note also in Table 1 that the column density ratio $N(\text{SiO})/N(\text{Si I})$ is a sensitive function of shock conditions varying between 20 (model 6 with low density and correspondingly low magnetic field) and 0.3 (model 4 at a high shock velocity). Hence in principle, one may be able to use observations of this ratio to discriminate between models.

It may be worth emphasising that our model requires shock velocities higher than roughly 30 km s^{-1} (the precise limit depends on the assumed magnetic field taken here to be 707 microgauss) in order to erode a sufficient quantity of silicon to explain the observations. Fig. 6 shows the sensitivity of both atomic silicon column density and line intensity to shock velocity. We note that previous models (e.g. Neufeld & Dalgarno 1989a,b) of the Orion shock have *assumed* the presence of a certain fraction of silicon in the gas phase in order to explain the available SiO observations. The present model is the first to consider the transition from solid to gas phase in the context of explaining observations of silicon-containing species in Orion-KL. This has been done using the sputtering yields computed by Field et al. (1997) and hence without recourse to a new ‘deus ex machina’.

The limits on the shock velocity derived above are somewhat dependent on the assumed magnetic field. In the models presented here, we have assumed the direction of the magnetic field to be transverse to the direction of shock propagation and thus we have not considered oblique shocks. However, one expects C-type shock structure to be weakly dependent upon the angle between the upstream magnetic field and the direction of shock propagation (Wardle & Draine, 1987). Our results therefore should hold in qualitative fashion for oblique shocks if the angle between the field and the shock normal is not too small (see Smith 1992 for further discussion).

The rate of sputtering of silicon in the shock depends on the relative velocities of charged grains and neutral species. This in turn depends on both the field strength and the shock velocities. In general, there exists a minimum magnetic field in order to permit the existence of a C-shock and a maximum magnetic field beyond which $v_i - v_n$, the relative ion-neutral velocity, becomes so small that the amount of silicon eroded into the gas becomes negligible. For intermediate values of B, $v_i - v_n$ reaches a maximum which is a large fraction of the shock velocity. To illustrate this, we show in Fig. 7 the column densities predicted by our model as a function of magnetic field at a shock velocity of 30 km s^{-1} and for a pre-shock density of $5 \times 10^5 \text{ cm}^{-3}$. One sees that in terms of such a model, the field must be less than 700 microgauss in order to maintain the Si I column density above 10^{15} cm^{-2} as required by the observations. This limit is however sensitively dependent upon the shock velocity (see Fig. 6) and one clearly needs to fit all available data to deduce parameters of the Orion shock.

Table 1. Column densities of Si I and other species calculated for a selection of C-shock models. Models 1 and 2 differ in that in model 2 we have considered dissociation of molecules subsequent to collision with grains. This process is neglected in all other models.

Model	n_H cm^{-3}	B μG	v_{sh} km s^{-1}	N(Si I) cm^{-2}	I(Si I)(2-1) $\text{erg cm}^{-2} \text{s}^{-1} \text{sr}^{-1}$	N(SiO) cm^{-2}	N(OH) cm^{-2}	N(H ₂ O) cm^{-2}	N(CO) cm^{-2}
1	$5 \cdot 10^5$	707	30	$1.2 \cdot 10^{15}$	$5.5 \cdot 10^{-5}$	$1.2 \cdot 10^{16}$	$6.0 \cdot 10^{14}$	$1.3 \cdot 10^{18}$	$9.7 \cdot 10^{17}$
2	$5 \cdot 10^5$	707	30	$6.8 \cdot 10^{15}$	$2.7 \cdot 10^{-4}$	$2.5 \cdot 10^{15}$	$9.3 \cdot 10^{15}$	$1.4 \cdot 10^{18}$	$8.7 \cdot 10^{17}$
3	$5 \cdot 10^5$	707	35	$1.9 \cdot 10^{16}$	$6.8 \cdot 10^{-4}$	$2.5 \cdot 10^{16}$	$8.1 \cdot 10^{14}$	$1.6 \cdot 10^{18}$	$9.6 \cdot 10^{17}$
4	$5 \cdot 10^5$	707	40	$6.6 \cdot 10^{16}$	$2.6 \cdot 10^{-3}$	$1.8 \cdot 10^{16}$	$1.1 \cdot 10^{15}$	$1.6 \cdot 10^{18}$	$9.4 \cdot 10^{17}$
5	$5 \cdot 10^5$	150	30	$3.8 \cdot 10^{16}$	$1.5 \cdot 10^{-3}$	$5.1 \cdot 10^{16}$	$8.0 \cdot 10^{14}$	$1.3 \cdot 10^{18}$	$3.1 \cdot 10^{17}$
6	10^5	316	30	$7.3 \cdot 10^{14}$	$2.1 \cdot 10^{-5}$	$1.5 \cdot 10^{16}$	$5.9 \cdot 10^{14}$	$1.1 \cdot 10^{18}$	$7.0 \cdot 10^{17}$

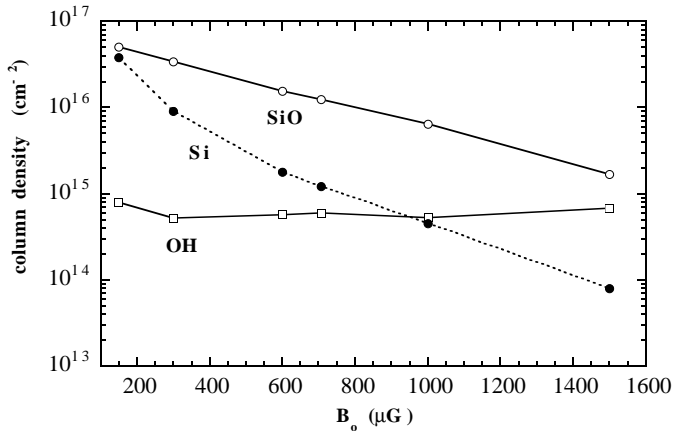


Fig. 7. Column densities of Si, SiO, and OH predicted by our C-shock calculations as a function of pre-shock magnetic field. The pre-shock hydrogen number density and shock velocity have been set to our standard values of $5 \cdot 10^5 \text{ cm}^{-3}$ and 30 km s^{-1} respectively.

6. Conclusions

We have used the Long Wavelength Spectrometer on board ISO to provide the first evidence for emission in the fine structure lines of atomic silicon. Our data show a feature at the wavelength of the J=2-1 $68.5 \mu\text{m}$ line with an intensity of $4.8 \cdot 10^{-5} \text{ erg s}^{-1} \text{ cm}^{-2} \text{ sr}^{-1}$ and a signal-to-noise ratio of 5.3. We find no evidence for the J=1-0 feature at $129 \mu\text{m}$ but this is not surprising given the conditions (temperature above 100 K) in Orion. We thus consider it likely that the J=2-1 line has been detected. After considering various possibilities, we have concluded that the line forms in the C-shock caused by the interaction of the outflows in the core of Orion-KL with surrounding ambient material. For a pre-shock gas density of $5 \cdot 10^5 \text{ cm}^{-3}$ (as e.g. in the models of Neufeld & Dalgarno 1989ab), we find that we need shock velocities larger than 30 km s^{-1} and magnetic fields of order a few hundred microgauss to explain the observed line intensity. These models use the sputtering yields computed by Field et al. (1997) and thus one can regard the detection of the $68.5 \mu\text{m}$ line as an indirect confirmation of these calculations.

Acknowledgements. We thank David Hollenbach, Paola Caselli, and David Flower for their comments on an early draft of this paper. We thank also Emmanuel Caux, Bruce Swinyard, and Sunil Sidher for their comments on the data reduction. CMW would like to thank the Institut d’Astrophysique de Paris for its hospitality during the initiation of this study. He also wishes to acknowledge travel support from ASI Grants ARS 66–96 and 98–116 as well as from the program “Dust and Molecules in Astrophysical Environments” financed by the MURST.

References

- Blake G.A., Sutton E.C., Masson C.R., Phillips T.G., 1987, *ApJ* 315, 621
 Brown J.M., Zink L.R., Evenson K.M., 1994, *ApJ* 423, L151
 Chernoff D.F., Hollenbach D.J., McKee C.F., 1982, *ApJ* 259, L97
 Draine B.T., Roberge W.G., 1982, *ApJ* 259, L91
 Field D., May P.W., Pineau des Forêts G., Flower D.R., 1997, *MNRAS* 285, 839
 Haas M.R., Hollenbach D.J., Erickson E.F., 1991, *ApJ* 374, 555
 Hollenbach D.J., McKee C.F., 1989, *ApJ* 342, 306
 Kaufman M.J., Hollenbach D.J., Tielens A.G.G.M., 1998, *ApJ* 497, 276
 Neufeld D., Dalgarno A., 1989a, *ApJ* 340, 869
 Neufeld D., Dalgarno A., 1989b, *ApJ* 344, 251
 Schilke P., Walmsley C.M., Pineau des Forêts G., Flower D.R., 1997, *A&A* 321, 293
 Schroeder K., Staemmler V., Smith M.D., Flower D.R., Jaquet R., 1991, *J. Phys. B.* 24, 2487
 Smith M.D., 1992, *ApJ* 390, 447
 Swinyard B.M., Burgdorf M., Clegg P.E., et al., 1998, *Proceedings of the SPIE Symposium Astronomical Telescopes and Instrumentation*. in press
 Trams N.R., Clegg P.E., Swinyard B.M., 1996, *Addendum to the LWS Observers manual*. SAI/96-166/Dc.
 Turner B.E., 1991, *ApJ* 376, 573
 Walmsley C.M., Pineau des Forêts G., Flower D.R., 1999, *A&A* 342, 542 (WPF)
 Wardle M., Draine B.T., 1987, *ApJ* 321, 321
 Wright M.C.H., Sandell G., Wilner D.J., Plambeck R.L., 1992, *ApJ* 393, 225
 Wright M.C.H., Plambeck R.L., Wilner D.J., 1996 *ApJ* 469, 216